Hindawi
Shock and Vibration
Volume 2024, Article ID 1451839, 19 pages
https://doi.org/10.1155/2024/1451839

Research Article

Dynamic Response Analysis of the Floor Structure under Random Crowd Excitation

Dong Cao[1,2], **Zuanfeng Pan**[1,2] **and Yu Fang**[3]

[1]*State Key Lab of Disaster Reduction in Civil Engineering, Tongji University, Shanghai 200092, China*
[2]*Department of Structural Engineering, Tongji University, Shanghai 200092, China*
[3]*Zhejiang Huayun Electric Power Engineering Design & Consultation Co., Ltd., Hangzhou, Zhejiang 310014, China*

Correspondence should be addressed to Zuanfeng Pan; zfpan@tongji.edu.cn

Received 2 February 2023; Revised 28 November 2023; Accepted 18 December 2023; Published 10 January 2024

Academic Editor: Jiaxi Zhou

The popularity of new structural systems and prestressing technology has led to the widespread use of the large-space floor structures in large buildings such as high-speed rail terminals, conference centers, and sports stadiums. The reduction of nonessential load-bearing elements and the increase in span of the structure result in a reduction in the natural frequency and damping ratio of the floor structure, while the floor is a crowded area with disorderly flow between people, which may lead to human-induced vibration problems. In order to assess the dynamic performance of the large-span floor structure under crowd load, the random crowd-floor vertical interaction equation is derived, and the correctness of the equation is verified by comparing it with the test. For the stochastic nature of walking crowds, a formulation modeling method for random crowd is proposed, including pedestrian-dynamics parameters, formulation model, and response parameters. The model is characterized by considering inter- and intrasubject variability and reflects the vertical interaction between pedestrians and the floor system. According to the random crowd-floor dynamic equation, the variation of modal parameters and acceleration response of the floor during random crowd walking are also analyzed. The research in this paper will help in analyzing the comfort of large-span floor structures under pedestrian excitation and better meet the needs of the development of lightweight large-span structures.

1. Introduction

In regard to the issue of human-induced vibration, the human-structure interaction (HSI) is usually considered, focusing on the analysis of structural dynamic response and pedestrian comfort. The appropriate human-structure coupling dynamic equation is the key to studying the problem of human-induced vibration. The complex footbridge is regarded as an Euler beam, which helps engineers estimate the change in structural acceleration under human-induced load so as to analyze the comfort index of footbridges. Specifications [1–4] provide a more detailed theory and operation method. For slender bridge structures, the transverse width of the bridge is much smaller than the length, so the influence of the width direction of the bridge can be ignored. However, for the floor structure, this assumption cannot be established, because the specification [5] clearly stipulates the aspect ratio of the one-way slab and the two-way slab. At the same time, because the simplified Euler beam only contains one-dimensional motion direction, it completely ignores the influence of lateral width. This simplification makes the movement of the crowd a linear motion. The simulation of random walking can only be considered based on the random distribution of pedestrian dynamic parameters, and the random mode of motion cannot be realized, which deviates from the actual situation.

An appropriate pedestrian model and mathematical model of walking load can better simulate the walking force exerted by pedestrians. Because the periodicity of a Fourier series model is more in line with the characteristics of pedestrian walking, it is favored by most researchers [6–9]. Some researchers put forward a load model for pedestrian walking speed [10]. Considering the randomness of walking load, the power spectrum model is more reasonable. Due to

different pedestrian weights and different walking styles, the inter- and intrasubject variability should not be ignored [11–13]. As is known to all, pedestrians walking on the structure is very complex. Due to human intelligence, pedestrians can catch up, cross, stay in place, and traverse, which further leads to the difficulty of crowd simulation. As the highest living creature, people can adaptively change their behavior according to the environmental changes. The current HSI effect only considers the influence of pedestrians walking on the structure [12, 14]. However, when the acceleration of the structure is too large, the annoyance rate of pedestrians increases, and pedestrians cannot maintain the original expected pace frequency. When pedestrians feel strong structural vibration, to maintain body balance, pacing frequency and phase will change adaptively under the self-regulation mechanism. Because this phenomenon can only be perceived by pedestrians when the structural vibration response exceeds the psychological limit, it is more challenging to study the intelligent behavior of pedestrians in the experiment [15, 16]. It should be noted that these elements are not mentioned in the current specification. The effect of randomness will be ignored when people are equivalent to a uniform load, which may cause the evaluation data to deviate from the actual situation.

For the description of the collective behavior of random crowds, the social force model is the most widely used pedestrian-dynamics model. The social force model includes the self-driving force generated by pedestrians being attracted by the target during walking, the interaction between pedestrians, and the repulsive force between pedestrians and obstacles [17, 18]. Fu and Wei [19] considered the inter- and intrasubject variability of the crowd and developed a new load model by associating the modified social force model with the walking force model. The applicability of the proposed method is demonstrated through specific concrete pedestrian bridges. Based on the social force model, Wei [20] studied the influence of the human-human interaction effect on crowd-induced load and structural response. The results show that the increase in pedestrian density is consistent with the decrease in average walking speed and pacing frequency of pedestrians in the crowd. The variability of pacing frequency between pedestrians also depends on the width of the walkway and the desired swing space of the pedestrian. Wei et al. [21] used the social force model to simulate crowd behavior, proposed a comprehensive method to quantify the uncertainty of the structural dynamics model and the crowd behavior, and then spread the various sources of uncertainty from the input parameters to the response of the footbridge.

Studies have shown that pedestrians walking and staying on the structure will lead to dynamic changes in structural frequency and damping ratio [12, 22–24]. Modal analysis and finite element analysis are widely used in human-induced vibration problems [22, 25–27], and these methods can effectively help identify the changes in structural dynamic parameters. The special biological structure characteristics of the human body will exert a damping effect on the structure to alleviate the existing vibration, which is like the vibration reduction effect of the tuned mass damper [28]. Due to the complex randomness of crowd behavior, the inter- and intrasubject variability will have a great impact on the structural response. However, the models used in engineering design so far are deterministic, and there is no framework modeling method for the stochastic crowd. Although the concepts of structural variability and uncertainty have been well developed, the human-structure interactions are still developing slowly.

Based on this, the vertical interaction equations for the human-floor system were derived in order to investigate the effect of stochastic crowd excitation on a large-span floor. The floor system is assumed to be simply supported on four sides. The influence of uncertainty in pedestrian dynamic parameters on structural modal parameters is analyzed. The framework theory of the random population model is studied, and the formula modeling method of the random population is given. The modeling method is characterized by considering both the influence of the lateral width of the floor system and the randomness of pedestrians. According to the calculation results of the model, from the perspective of comfort, the pedestrian distribution law of the floor at the maximum acceleration time is given.

2. Theoretical Analysis

In order to simplify the analysis, only four-sided simple supports are considered for the floor system and do not consider the composite laminated plate. The rectangular thin plate is considered to have damping. The pedestrian body always keeps contact with the thin plate while walking or standing.

2.1. Formulations. The dynamic equation of a rectangular thin plate with damping is expressed as follows [29]:

$$D\left[\nabla^4 W(x,y,t) + \chi\nabla^4\frac{\partial W(x,y,t)}{\partial t}\right] + \rho h\frac{\partial W^2(x,y,t)}{\partial t^2} = F(x,y,t). \tag{1}$$

D is the bending stiffness of the plate:

$$D = \frac{Eh^3}{12\left(1-\nu^2\right)}, \tag{2}$$

where E is the elastic modulus of the material, h is the effective plate thickness, and ν is Poisson's ratio. $W(x, y, t)$ is the vertical deflection of the plate and χ represents the damping of the plate. According to the theory of viscoelasticity, $\chi = 2\xi\omega$ is generally adopted [29], ξ is the damping ratio of the structure, and ω is the circular frequency of the structure. In particular, $\omega_{mn} = \pi^2(i^2/a^2 + j^2/b^2)\sqrt{D/\rho h}$, and ρ is the plate density. $F(x, y, t)$ is the excitation load on the plate, and ∇^4 represents quadratic Laplacian operator, which can be rewritten as follows:

$$\nabla^4 = \frac{\partial^4}{\partial x^4} + 2\frac{\partial^4}{\partial x^2\partial y^2} + \frac{\partial^4}{\partial y^4}. \tag{3}$$

According to the mode decomposition method [30],

$$W(x,y,t)=\sum_{m=1}^{\infty}\sum_{n=1}^{\infty}\varphi_{mn}(x,y)q_{mn}(t). \tag{4}$$

Equation (1) is rewritten as follows:

$$D\left[\nabla^4\sum_{m=1}^{\infty}\sum_{n=1}^{\infty}\varphi_{mn}(x,y)q_{mn}(t)+\chi\sum_{m=1}^{\infty}\sum_{n=1}^{\infty}\varphi_{mn}(x,y)\dot{q}_{mn}(t)\right]+\rho h\sum_{m=1}^{\infty}\sum_{n=1}^{\infty}\varphi_{mn}(x,y)\ddot{q}_{mn}(t)=F(x,y,t), \tag{5}$$

where ϕ_{mn} is the vibration mode of the floor, the vibration mode of the simply supported plate on four sides $\varphi_{mn}(x,y)=\sin m\pi x/a\sin n\pi y/b$, and q_{mn} is the generalized coordinate.

When the plate vibrates freely, the load term $F(x,y,t)=0$, separating the variables from equation (5). Similarly, referring to the treatment method of the simply supported beam equation [31], the ratio of the equation can be defined as $-\omega_{mn}^2$:

$$\frac{\ddot{q}_{mn}(t)}{q_{mn}(t)+\chi\dot{q}_{mn}(t)}=\frac{D\nabla^4\varphi_{mn}(x,y)}{\rho h\varphi_{mn}(x,y)}=-\omega_{mn}^2. \tag{6}$$

Hence,

$$\begin{cases}\ddot{q}_{mn}(t)+\chi\omega_{mn}^2\dot{q}_{mn}(t)+\omega_{mn}^2q_{mn}(t)=0,\\ D\nabla^4\varphi_{mn}(x,y)-\rho h\omega_{mn}^2\varphi_{mn}(x,y)=0.\end{cases} \tag{7}$$

Then, equation (5) becomes as follows:

$$\rho h\sum_{m=1}^{\infty}\sum_{n=1}^{\infty}\omega_{mn}^2\varphi_{mn}(x,y)\left[q_{mn}(t)+\chi\dot{q}_{mn}(t)\right]+\rho h\sum_{m=1}^{\infty}\sum_{n=1}^{\infty}\varphi_{mn}(x,y)\ddot{q}_{mn}(t)=F(x,y,t). \tag{8}$$

Equation (8) is left-multiplied by the floor mode $\varphi_{mn}(x,y)$ and integrated along the x and y directions of the plate. According to the orthogonality of the plate,

$$M_{mn}\ddot{q}_{mn}(t)+M_{mn}\chi\omega_{mn}^2\dot{q}_{mn}(t)+M_{mn}\omega_{mn}^2q_{mn}(t)=P_{mn}(x,y,t), \tag{9}$$

where the generalized force $P_{mn}(x,y,t)=\iint_S F(x,y,t)\varphi_{mn}(x,y)\mathrm{ds}$, and generalized mass $M_{mn}(x,y,t)=\rho h\iint_S\varphi_{mn}^2(x,y)\mathrm{ds}$.

The mass-spring-damper (MSD) model simplifies the pedestrian body into concentrated mass m_P, additional stiffness k_P, and damping c_P. This model has been adopted by many researchers [22, 26, 32] and can better reflect HSI effect.

It is assumed that the displacement of the pedestrian staying on the structure is $Z(t)$, as shown in Figure 1. The human-structure vertical coupling system, due to the structural vibration and the continuous walking of pedestrians, will produce relative displacement between them. Considering the continuity of time, there are relative velocity differences and relative acceleration differences between the structure and pedestrians. The relative acceleration makes the pedestrian body subject to the inertial force $P_g(t)$ generated by the mass m_P. In addition, the relative velocity will cause the pedestrian to suffer the damping force $P_c(t)$, and the relative displacement will make the pedestrian subject to the elastic force $P_k(t)$:

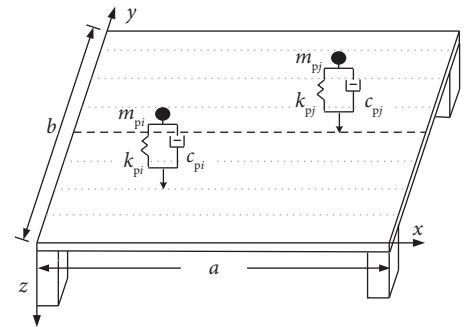

Figure 1: Rectangular thin plate and mass-stiffness-damping model.

$$P_{\mathrm{g}}(t)=M_{\mathrm{p}}\ddot{Z}(t), \tag{10}$$

$$P_{\mathrm{k}}(t)=k_{\mathrm{p}}\left[W(x,y,t)-Z(t)\right]_{x=l_x,y=l_y}. \tag{11}$$

Here, coordinates (l_x, l_y) indicate the position of pedestrians in x and y directions on the floor.

$$P_{\mathrm{c}}(t)=c_{\mathrm{p}}\left[\frac{\mathrm{d}W(x,y,t)}{\mathrm{d}t}-\dot{Z}(t)\right]_{x=l_x,y=l_y}. \tag{12}$$

It is worth noting that the derivative term in $P_c(t)$ is

$$\frac{\mathrm{d}W(x,y,t)}{\mathrm{d}t}=\frac{\partial W(x,y,t)}{\partial x}\frac{\mathrm{d}x}{\mathrm{d}t}+\frac{\partial W(x,y,t)}{\partial y}\frac{\mathrm{d}y}{\mathrm{d}t}+\frac{\partial W(x,y,t)}{\partial t}, \tag{13a}$$

$$\frac{\partial W(x,y,t)}{\partial x}\frac{\mathrm{d}x}{\mathrm{d}t}=\frac{\partial W(x,y,t)}{\partial x}v_x, \tag{13b}$$

$$\frac{\partial W(x,y,t)}{\partial y}\frac{\mathrm{d}y}{\mathrm{d}t}=\frac{\partial W(x,y,t)}{\partial y}v_y. \tag{13c}$$

In fact, the additional velocity caused by the change of load is small in both the x and y directions, which can be ignored. Therefore, equation (13a) is simplified as follows:

$$\frac{\mathrm{d}W(x,y,t)}{\mathrm{d}t}\approx\frac{\partial W(x,y,t)}{\partial t}. \tag{14}$$

Due to the influence of HSI, the excitation of the structure is changed into

$$F(x,y,t)=\left\{k_{\mathrm{p}}[Z(t)-W(x,y,t)]+c_{\mathrm{p}}\left[\dot{Z}(t)-\frac{\partial W(x,y,t)}{\partial t}\right]+\mathrm{g}_{\mathrm{p}}(t)\right\}\delta(x-l_x)\left(y-l_y\right), \tag{15}$$

where δ is the Dirichlet function, which means that the pedestrian will generate the corresponding excitation only at a certain point. $g_{\mathrm{p}}(t)$ is the walking force generated by pedestrian walking.

The mode decomposition method is introduced in equation (15).

$$F(x,y,t)=\left\{k_{\mathrm{p}}\left[Z(t)-\sum_{m=1}^{\infty}\sum_{n=1}^{\infty}\varphi_{mn}(x,y)q_{mn}(t)\right]+c_{\mathrm{p}}\left[\dot{Z}(t)-\sum_{m=1}^{\infty}\sum_{n=1}^{\infty}\varphi_{mn}(x,y)\dot{q}_{mn}(t)\right]+\mathrm{g}_{\mathrm{p}}(t)\right\}\delta(x-l_x)\left(y-l_y\right). \tag{16}$$

According to the dynamic balance relationship, the equilibrium conditions of the pedestrian subjected to inertial force, elastic force, and damping force are as follows:

$$\begin{aligned}&m_{\mathrm{p}}\ddot{Z}(t)+k_{\mathrm{p}}[Z(t)-W(x,y,t)]\\&+c_{\mathrm{p}}\left[\dot{Z}(t)-\frac{\partial W(x,y,t)}{\partial t}\right]=0.\end{aligned} \tag{17}$$

The pedestrian dynamic equation can be obtained by substituting equation (4) into equation (17):

$$\begin{aligned}&m_{\mathrm{p}}\ddot{Z}(t)+c_{\mathrm{p}}\dot{Z}(t)+k_{\mathrm{p}}Z(t)-c_{\mathrm{p}}\sum_{m=1}^{\infty}\sum_{n=1}^{\infty}\varphi_{mn}\left(l_x,l_y\right)\dot{q}_{mn}(t)\\&-k_{\mathrm{p}}\sum_{m=1}^{\infty}\sum_{n=1}^{\infty}\varphi_{mn}\left(l_x,l_y\right)q_{mn}(t)=0.\end{aligned} \tag{18}$$

Equation (17) can be further transformed into

$$k_{\mathrm{p}}[Z(t)-W(x,y,t)]+c_{\mathrm{p}}\left[\dot{Z}(t)-\frac{\partial W(x,y,t)}{\partial t}\right]=-m_{\mathrm{p}}\ddot{Z}(t). \tag{19}$$

Therefore, equation (16) is simplified as

$$F(x,y,t)=\left[\mathrm{g}_{\mathrm{p}}(t)-m_{\mathrm{p}}\ddot{Z}(t)\right]\delta(x-l_x)\left(y-l_y\right). \tag{20}$$

The generalized force $P_{mn}(x, y, t)$ can be simplified as

$$\begin{aligned}P_{mn}(x,y,t)&=\iint_S F(x,y,t)\varphi_{mn}(x,y)\mathrm{d}s,\\&=\iint_S\left[f_{\mathrm{p}}(t)-m_{\mathrm{p}}\ddot{Z}(t)\right]\varphi_{mn}(x,y)\delta(x-l_x)\left(y-l_y\right)\mathrm{d}s,\\&=\left[\mathrm{g}_{\mathrm{p}}(t)-m_{\mathrm{p}}\ddot{Z}(t)\right]\varphi_{mn}(x,y).\end{aligned} \tag{21}$$

The dynamic equilibrium equation of plate can be obtained by substituting the above equation into equation (9):

$$\begin{aligned}&M_{mn}\ddot{q}_{mn}(t)+m_{\mathrm{p}}\varphi_{mn}\left(l_x,l_y\right)\ddot{Z}(t)+M_{mn}\chi\omega_{mn}^2\dot{q}_{mn}(t)\\&+M_{mn}\omega_{mn}^2q_{mn}(t)=\mathrm{g}_{\mathrm{p}}(t)\varphi_{mn}\left(l_x,l_y\right).\end{aligned} \tag{22}$$

The coupling equation considering HSI effect can be obtained by equations (18) and (22).

$$\mathbf{M}\ddot{\mathbf{U}}+\mathbf{C}\dot{\mathbf{U}}+\mathbf{K}\mathbf{U}=\mathbf{F}. \tag{23}$$

It is assumed that there are j pedestrians in the structure, the first N order of the structure is taken for analysis. Matrix **M**, **C**, and **K** are expressed by the following block matrices:

$$\begin{aligned}
\mathbf{M}11 &= \mathrm{diag}\left[M_{mn}\right]_{N\times N},\\
\mathbf{M}22 &= \mathrm{diag}\left[m_{pj}\right]_{j\times j},\\
\mathbf{M}12 &= \begin{pmatrix} m_{p1}\varphi_{11} & \cdots & m_{pj}\varphi_{11} \\ \vdots & \ddots & \vdots \\ m_{p1}\varphi_{mn} & \cdots & m_{pj}\varphi_{mn} \end{pmatrix}_{j\times N},
\end{aligned} \tag{23a}$$

$$\begin{aligned}
\mathbf{K}11 &= \mathrm{diag}\left[M_{mn}\omega_{mn}^2\right]_{N\times N},\\
\mathbf{K}22 &= \mathrm{diag}\left[k_{pj}\right]_{j\times j},\\
\mathbf{K}21 &= \begin{pmatrix} -k_{p1}\varphi_{11} & \cdots & -k_{p1}\varphi_{mn} \\ \vdots & \ddots & \vdots \\ -k_{pj}\varphi_{11} & \cdots & -k_{pj}\varphi_{mn} \end{pmatrix}_{j\times N},
\end{aligned} \tag{23b}$$

$$\begin{aligned}
\mathbf{C}11 &= \mathrm{diag}\left[2M_{mn}\xi_{mn}\omega_{mn}\right]_{N\times N},\\
\mathbf{C}22 &= \mathrm{diag}\left[c_{pj}\right]_{j\times j},\\
\mathbf{C}21 &= \begin{pmatrix} -c_{p1}\varphi_{11} & \cdots & -c_{p1}\varphi_{mn} \\ \vdots & \ddots & \vdots \\ -c_{pj}\varphi_{11} & \cdots & -c_{pj}\varphi_{mn} \end{pmatrix}_{j\times N},
\end{aligned} \tag{23c}$$

$$\mathbf{F} = \left[\sum_{i=1}^{j} \mathrm{g}_{pi}(t)\varphi_{11} \cdots \sum_{i=1}^{j} \mathrm{g}_{pi}(t)\varphi_{mn}\ 0 \cdots 0\right], \tag{23d}$$

$$\begin{aligned}
\mathbf{M} &= \begin{bmatrix} \mathbf{M11} & \mathbf{M12} \\ \mathbf{0} & \mathbf{M22} \end{bmatrix},\\
\mathbf{C} &= \begin{bmatrix} \mathbf{C11} & \mathbf{0} \\ \mathbf{C21} & \mathbf{C22} \end{bmatrix},\\
\mathbf{K} &= \begin{bmatrix} \mathbf{K11} & \mathbf{0} \\ \mathbf{K21} & \mathbf{K22} \end{bmatrix}.
\end{aligned} \tag{23e}$$

When the floor system is simply supported on the short side and freely constrained on the long side, equation (23) degenerates into one-dimensional dynamic equation, and the mode shape of simply supported beam is [31]

$$\varphi_x = \sin\frac{i\pi}{L}x, \tag{24}$$

where L is the long side length of the plate. As shown in Figure 2, the general bridge structure can be approximately solved by substituting equation (24) into equation (23).

For the above nonproportional damping time-varying differential equation, the state space method is used to solve the modal characteristics of the time-varying system, and the variable step size fourth-order five-stage Runge–Kutta–Felhberg algorithm is used to solve its dynamic response. Equation (23) can be rewritten as a state space expression to solve changes in the modal frequency and damping ratio of the floor [22]:

$$\dot{\mathbf{V}} = \mathbf{A}\mathbf{V} + \mathbf{B}, \tag{25}$$

with $\dot{\mathbf{V}} = \begin{Bmatrix} \mathbf{U} \\ \dot{\mathbf{U}} \end{Bmatrix}$; $\mathbf{A} = \begin{bmatrix} \mathbf{0} & \mathbf{I} \\ -\mathbf{M}^{-1} & -\mathbf{M}^{-1}\mathbf{C} \end{bmatrix}$; $\mathbf{B} = \begin{Bmatrix} \mathbf{0} \\ \mathbf{M}^{-1}\mathbf{F}(t) \end{Bmatrix}$.

Here, $\mathbf{I}$ denotes the identity matrix with the same dimension as those for mass, stiffness, and damping of the system and $F(t)$ is the force vector. The modal properties can be obtained by solving the following eigenvalue problem:

$$\mathbf{A}\varphi = \lambda\varphi, \tag{26}$$

where λ and ϕ stand for the complex eigenvalue and its corresponding eigenvector. For a damped multidegree-of-freedom (MDOF) system, the jth frequency, f_j, and the damping ratio, ξ_j, corresponding to each DOF are given as follows:

$$f_j = \frac{\left|\lambda_j\right|}{2\pi};\ \xi_j = \frac{\left|\mathrm{Re}\left(\lambda_j\right)\right|}{\left|\lambda_j\right|}. \tag{27}$$

2.2. Model Validation. In order to verify the accuracy of the human-floor coupling equation, the numerical solution is compared with the experimental data. The plane size is 5 m × 8 m, the span is 7.7 m and 4.7 m, respectively, and the plate thickness is 60 mm. It is a typical composite steel-concrete floor structure. The first three modal frequencies of the floor are 4.55 Hz, 9.0 Hz, and 11.8 Hz; the corresponding damping ratios are 0.84%, 0.88%, and 0.84% [33]. For the simply supported beam structure, the size is 11.2 m × 2 m [23, 34]. The actual area is 10.8 m × 2 m, the first three natural frequencies of the beam are 4.44 Hz, 16.8 Hz, and 26.1 Hz, respectively. The modal mass of each order remains 7128 kg.

Results of the standing test and theoretical calculations are shown in Table 1. The pedestrians weight varies between 50 kg and 80 kg. The data in brackets are calculated according to equations (23a)–(23e). Comparing the measured results of the floor system, it can be found that the calculated values are close to the experimental values. The calculation error of the modal frequency is less than 1%, and the difference in the modal damping ratio is less than 7%.

12 pedestrians are selected to further analyze the influence on pedestrian walking. The values of the natural frequency, damping ratio, and average pedestrian weight for each test are shown in Table 2. No. B-1 to No. B-3 are parameters identified by the test, and No. B-4 to No. B-8 are calculated modal parameters. It can be seen from Figure 3 that the experimental values of the modal damping ratio fall within the calculated effective range, and the modal frequency is close to the calculated values. In Figure 3, f_{s1} is the first modal frequency of the structure, m_{s1} is the modal mass, ξ_s is the damping ratio, c_s and k_s are the calculated structural damping and stiffness. The difference in modal frequency is less than 1% for 10 pedestrians walking.

Table 3 shows the modal damping ratio and modal frequency variation values of the coupling system for pedestrians standing on the footbridge. When 10 pedestrians are standing at the mid-span of the footbridge, the modal damping calculated by the SDOF model is 3.4%, which is higher than the 2.6% measured by the test value. Since the

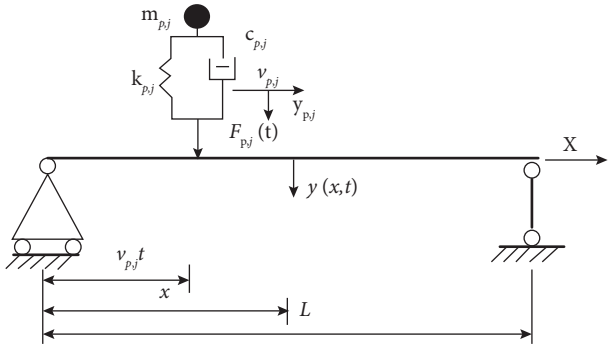

Figure 2: Simply supported beam model.

Table 1: Influence of standing mode on floor modal parameters.

No.	Pedestrian parameters [33]						Floor parameters	
	Gender	Weight (kg)	f_H (Hz)	ξ_p (%)	c_p (N·s/m)	k_p (N/m)	f_{os} (Hz)	ξ_p (%)
A1	Female	49.4	5.22	32.08	1039	53141	4.523 (4.523)	1.30 (1.27)
A2	Female	54.5	5.19	31.80	1130	57955	4.520 (4.520)	1.36 (1.33)
A3	Female	60.9	5.30	32.90	1334	67535	4.517 (4.516)	1.35 (1.33)
A4	Male	59.1	4.89	39.65	1440	55791	4.520 (4.524)	1.47 (1.36)
A5	Male	70	5.08	44.66	1996	71316	4.517 (4.518)	1.40 (1.35)
A6	Male	80.5	5.18	41.30	2164	85274	4.511 (4.511)	1.47 (1.43)

Table 2: Dynamic parameters of pedestrians.

No.	Pedestrians	Location	Average weight (kg)	f_P (Hz)		ξ_p (%)	
				Min	Max	Min	Max
B1	3	Mid-span	70	2.75	3.25	25.0	35.0
B2	6	Mid-span	70	2.75	3.25	25.0	32.5
B3	10	Mid-span	70	2.25	3.00	25.0	30.0
B4	1	Mid-span	70	2.75	3.25	25.0	35.0
B5	3	Mid-span	70	2.75	3.25	25.0	35.0
B6	6	Mid-span	70	2.75	3.25	25.0	32.5
B7	10	Mid-span	70	2.25	3.00	25.0	30.0
B8	12	Mid-span	70	2.25	3.00	25.0	30.0

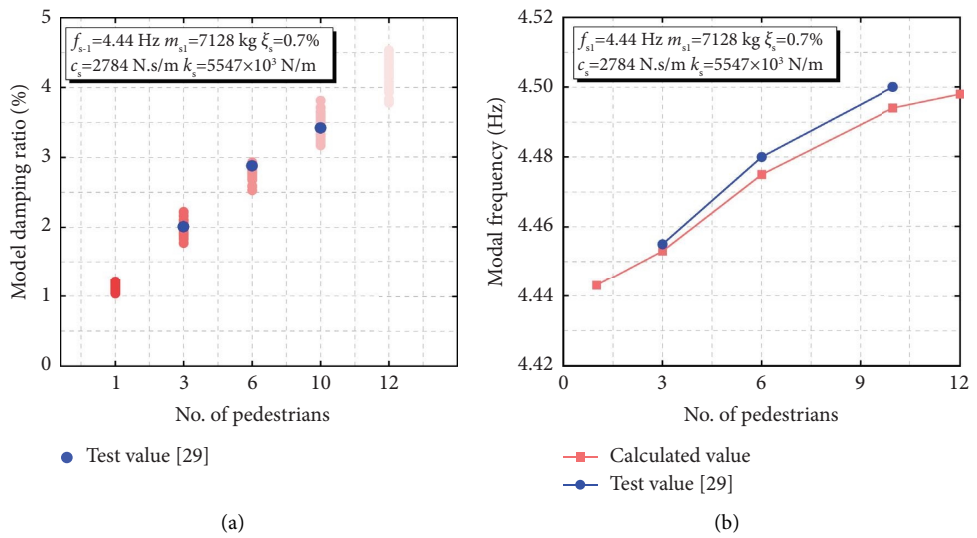

Figure 3: Pedestrians walking mode verification. (a) Modal damping ratio and (b) modal frequency.

influence of lateral width is considered in this paper, it is assumed that pedestrians are orderly distributed near the mid-span of the structure, and the distribution distance and arrangement mode are shown in reference [35]. According to Table 3, the error between the calculation results and test values is smaller when 3 and 6 pedestrians stand, and the modal frequency calculation results of 10 pedestrians standing are closer to the test values than the SDOF model.

3. Pedestrian Parameter Analysis

3.1. Parameter Values. In the process of pedestrians walking, the body gravity center is constantly changing, so the dynamic parameters of pedestrians in the standing and walking state are different. The average human natural frequency was 5.24 Hz (±0.4 Hz), and the average human damping was 0.39 (±0.05) [35]. When a single person stands on the structure, the natural frequency of the standing posture is recommended to be 5.12 Hz, and the average damping ratio is recommended to be 36.76% [32]. For pedestrians in the walking mode, considering the HSI effect, the vertical natural frequency of pedestrian in the SDOF model should be 2.75 Hz–3 Hz and the damping ratio 27.5%–30% [23]. In the vibration response analysis of reference [22], the damping and stiffness coefficients of pedestrians are 612 N·s/m and 14110 N/m, respectively. Silva and Pimentel [36] proposed the equivalent calculation formula for dynamic parameters of the SDOF pedestrian model:

$$\begin{aligned} \overline{m}_{\mathrm{p}} &= 97.082 + 0.275 m_{\mathrm{p}} - 37.518 f_{\mathrm{p}}, \\ \overline{c}_{\mathrm{p}} &= 29.041 \overline{m}_{\mathrm{p}}^{\,0.883}, \\ \overline{k}_{\mathrm{p}} &= 30351.744 - 50.261 \overline{c}_{\mathrm{p}} + 0.035 \overline{c}_{\mathrm{p}}^{2}, \end{aligned} \tag{28}$$

where $\overline{m}_{\mathrm{p}}$, $\overline{c}_{\mathrm{p}}$, and $\overline{k}_{\mathrm{p}}$ are equivalent mass, equivalent damping, and equivalent stiffness, respectively. According to the calculation, the dynamic parameters of the equivalent conversion for pedestrian walking are smaller than those for pedestrian standing. The pedestrian standing parameters in Section 3.2 and Section 3.3 are the same as those in the literature [35], and the values of the pedestrian walking parameters are the same as those in the literature [23].

According to the observation of pedestrian walking speed under different crowd densities on the high-speed rail platform, 2277 sets of measured data were statistically analyzed in the literature [37], and the results are shown in Table 4.

3.2. Stiffness Parameters. In the numerical analysis, the pedestrian weight is 60 kg–80 kg, and the damping is 1700 N·s/m when the pedestrian stands. When pedestrians walk, the damping is 750 N·s/m and the stiffness range is 6×10^4 N/m–8×10^4 N/m. The specific conversion method for the pedestrian dynamic parameters is as follows:

$$f_{\mathrm{p}} = \frac{1}{2\pi} \sqrt{\frac{k_p}{m_p}}, \tag{29}$$

$$\xi_{\mathrm{p}} = \frac{c_p}{2\sqrt{k_p m_p}}, \tag{30}$$

where f_p and ξ_p are the vertical natural frequency and damping ratio of pedestrians. m_p, c_p, and k_p are the pedestrian weight, damping, and stiffness, respectively.

It can be seen from Figure 4(a) that compared to the structural initial state, the modal damping ratio increases overall, but the amplitude of the rise is inversely related to the pedestrian stiffness. The increase in pedestrian stiffness will lead to a decrease in the floor damping ratio. At the same time, with the decrease in pedestrian weight, the inverse correlation is more obvious. It can be seen from Figure 4(b) that the floor modal frequency is inversely correlated with the pedestrian stiffness, and with the increase in pedestrian weight, the inverse correlation is more obvious. However, for the 75 kg and 80 kg pedestrians, when the stiffness is taken as 6×10^4 N/m and 6.5×10^4 N/m, the decrease in the floor frequency is lower than that of the 60 kg pedestrian. Results show that when the pedestrian stiffness is low, the change in structural frequency is not absolutely dependent on the human-structure mass ratio for pedestrian standing, but may be related to the values of pedestrian stiffness and weight at the same time.

The distribution range of pedestrian stiffness in the walking state is 1.8×10^4 N/m–3×10^4 N/m [23]. The real-time changes of the floor structure dynamic parameters when the pedestrian steps at 2.0 Hz, with a damping of 1700 N·s/m and a weight of 70 kg are shown in Figure 5. The trend for both floor damping ratio and frequency increases and then decreases, reaching a maximum at the mid-span position. In order to further analyze the influence of pedestrian weight change, the peak values of the floor time-varying frequency and time-varying damping ratio are taken for analysis. It can be seen from Figure 6 that the changes in the floor modal damping ratio and frequency are positively correlated with the pedestrian stiffness for walking state. The smaller the pedestrian weight is, the greater the increase range of the floor modal damping ratio, but the smaller the increase range of the floor modal frequency.

3.3. Damping Parameters. The influence of pedestrian damping on the dynamic parameters when standing is shown in Figure 7. When the pedestrian weight is constant and the pedestrian damping is increasing, the amplitude of the increase in the floor modal damping ratio decreases. The larger the weight, the more obvious the HSI effect. For the change in the floor modal frequency, it can be seen from Figure 7(b) that when the pedestrian damping is the same and the weight is greater, the floor modal frequency is smaller. With the increase in pedestrian damping, the floor modal frequency increases, but it is still less than the original frequency.

It can be seen from Figure 8 that when pedestrians with the same weight (70 kg) and the same stiffness (75000 N/m) walk through the floor completely, the floor modal damping ratio and the floor modal frequency significantly increase. The rising rate of the floor modal damping ratio is positively correlated with the pedestrian damping, and the rising rate of the modal frequency is inversely correlated with the

Table 3: Verifications of pedestrians standing on the footbridge.

Pedestrians	Test value [34]		SDOF model		Present	
	f_{os} (Hz)	ξ_p (%)	f_{os} (Hz)	ξ_p (%)	f_{os} (Hz)	ξ_p (%)
0	4.440	0.60	4.440	0.60	4.440	0.60
3	4.363	1.35	4.359	1.47	4.360	1.46
6	4.259	2.30	4.265	2.62	4.282	2.46
10	4.175	2.60	4.174	3.40	4.237	3.04

Table 4: The mean values and standard deviations of the pacing frequency.

Crowd density (p/m^2)	No. of pedestrians (p)	Mean frequency (Hz)	Standard deviation (Hz)
0.5	533	1.8834	0.1794
0.75	461	1.8197	0.1727
1.0	389	1.7220	0.1321
1.25	253	1.6399	0.0711
1.5	256	1.4380	0.0560
1.75	207	1.3812	0.0227
2	178	1.3471	0.0111

Note. people/m^2 is simplified as p/m^2.

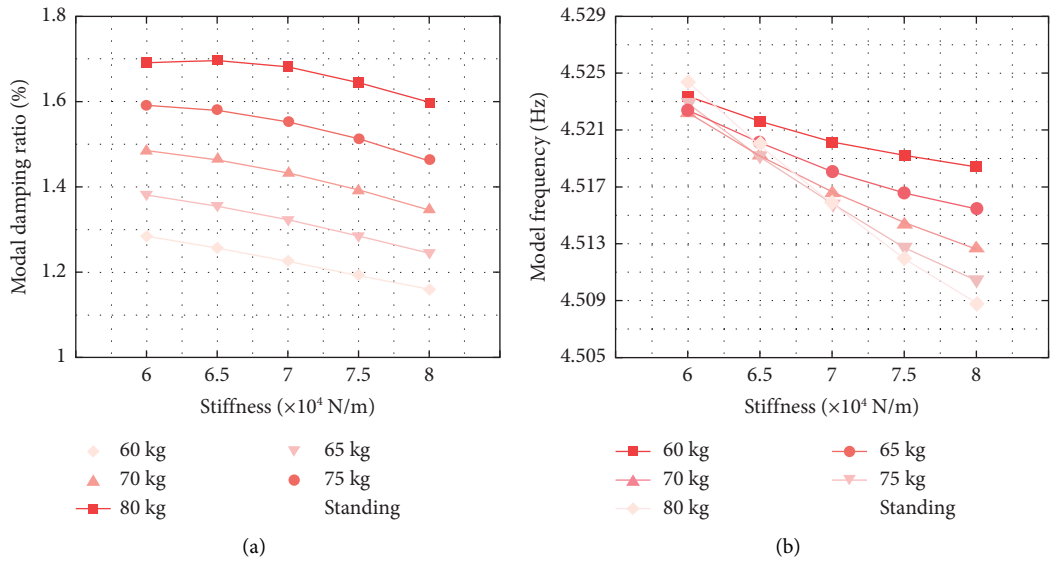

Figure 4: The influence of pedestrian stiffness on structural modal parameters in pedestrian standing state. (a) Modal damping ratio and (b) modal frequency.

pedestrian damping. It can be seen from Figure 9(a) that the higher the pedestrian weight is, the smaller the rise range of the floor modal damping ratio is. In particular, for a pedestrian of 60 kg, when the damping coefficient increases from 850 N·s/m to 950 N·s/m, the increase in amplitude of the floor modal damping ratio begins to decrease. By comparing and analyzing the influence of pedestrian stiffness change on the floor modal damping ratio in Figure 6(a), it can be found that considering the HSI effect, the influence of pedestrian weight and pedestrian damping should be considered. It can be found from Figure 9(b) that the modal frequency decreases approximately linearly with the pedestrian damping. Compared with the initial vertical natural frequency of 4.55 Hz, the floor modal frequency increases at 550 N·s/m and 650 N·s/m, and decreases with the increase of pedestrian damping.

4. Random Pedestrian Framework

4.1. Framework Model. The floor structure is a composite floor system, and the parameters are the same as those in Section 2.2. It is assumed that the pedestrian weight is 70 kg [23], the stiffness is 25000 N/m, the damping is 950 N·s/m, and the step frequency range is 1.8 Hz–2.2 Hz [8, 22]. It is assumed that the deterministic crowd walks along the long side of the mid-span at a constant pacing frequency, and the change trends of the floor modal parameters are shown in Figure 10. When the pedestrian

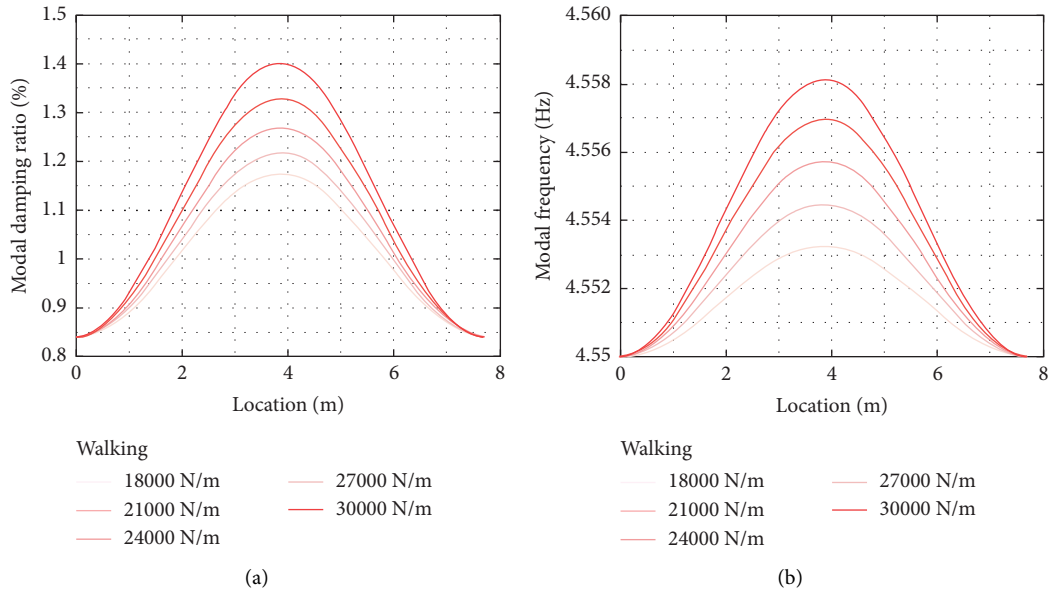

Figure 5: Real-time changes of structural dynamic parameters under pedestrian walking with different stiffness.

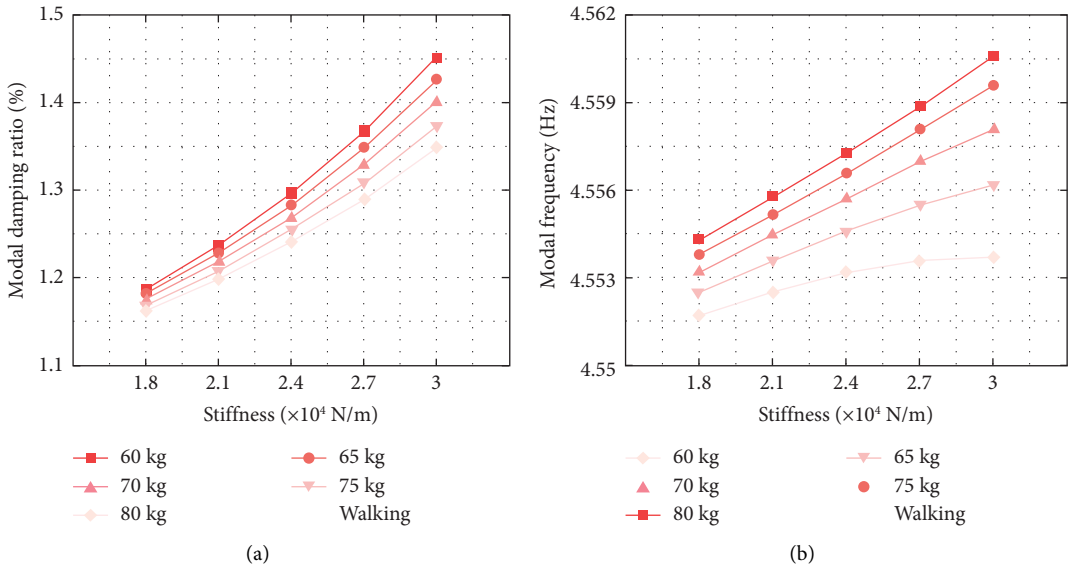

Figure 6: The influence of pedestrian stiffness on structural modal parameters in pedestrian walking state. (a) Modal damping ratio and (b) modal frequency.

dynamic parameters are determined, changes in the floor modal parameters will have nothing to do with the pacing frequency. This is because when the pacing frequency is determined, only the walking speed will be affected, and finally, only the time difference of the crossing structure will result. Therefore, considering the randomness of pedestrian walking, it is more reasonable than deterministic pedestrian [15].

In order to realize the formulaic model of a random crowd walking on a long-span floor, the modeling process is divided into dynamic parameter preparation, formulaic modeling, and response analysis. The detailed steps can be referred to Figure 11.

4.1.1. Dynamic Parameters. The number of pedestrians under different crowd densities is determined by the span of the structure. The pedestrian weight obeys a normal distribution, with an average value of 75 kg and a standard deviation of 15 kg [12]. The vertical natural vibration frequency of pedestrians standing is 4.84 Hz–5.64 Hz, and the damping ratio is 34–44% [35]. The natural vibration frequency of pedestrian walking is 2.75 Hz–3 Hz, and the damping ratio is 27.5–30% [23]. The corresponding damping and stiffness are calculated according to equations (29) and (30). The pedestrian pacing frequency follows a normal distribution [37], and the floor described in Section 2.3 is selected as the structure for analysis.

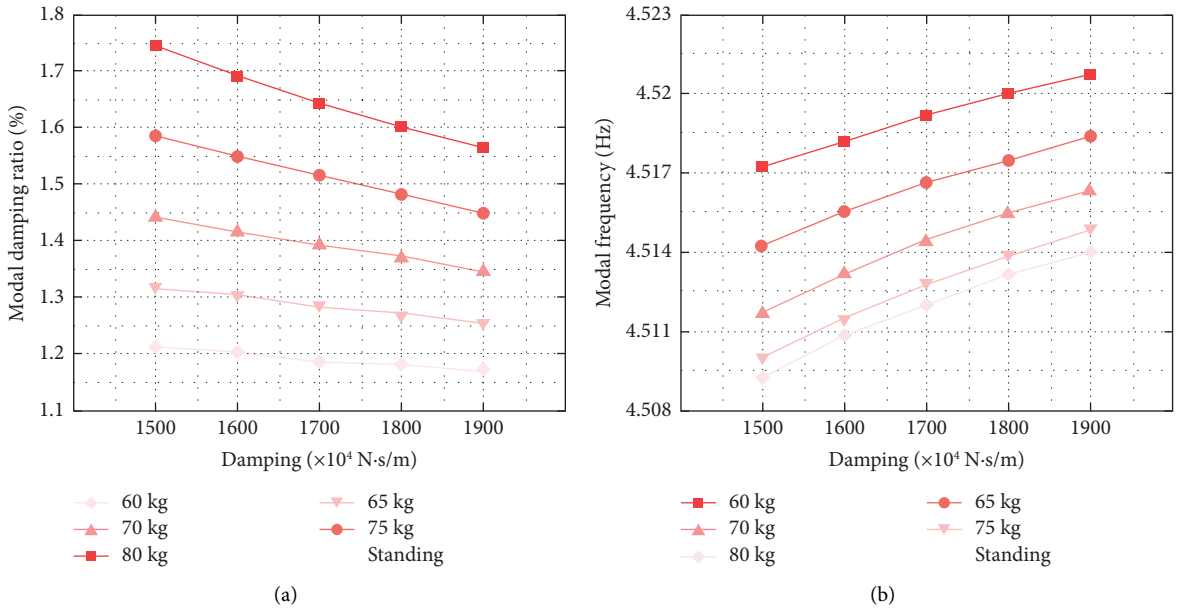

Figure 7: The influence of pedestrian damping on structural modal parameters in pedestrian standing state. (a) Modal damping ratio and (b) modal frequency.

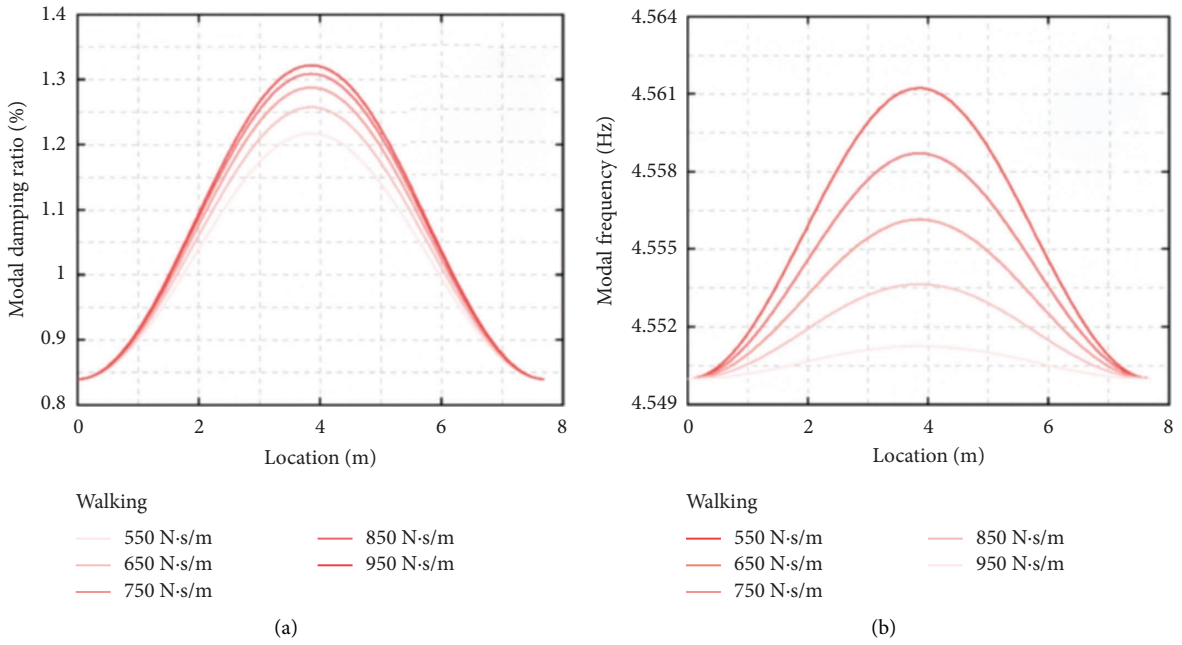

Figure 8: Real-time changes of structural dynamic parameters under pedestrian walking with different damping.

4.1.2. Formulaic Modeling. The mass matrix **M**, damping matrix **C**, and stiffness matrix **K** of pedestrians are generated, respectively. The pedestrian weight, vertical natural frequency, and pacing frequency are random.

(a) The pacing frequency of each step is used to calculate the time of each step: $T_j^k = (f_{pj}^k)^{-1}$. f_{pj}^k is the k_{th} pacing frequency of pedestrian j.

(b) The relationship between pacing frequency and pacing speed follows $f_{pj}^k = 0.35(V_j^k)^3 - 1.59(V_j^k)^2 + 2.93V_j^k$ [38], where V_j^k represents the k_{th} step speed of pedestrian j. The pacing length of each step is calculated by using the relationship $l_j^k = V_j^k \cdot T_j^k$.

(c) In the standing state, the position of pedestrians is fixed. Considering the actual width of the human

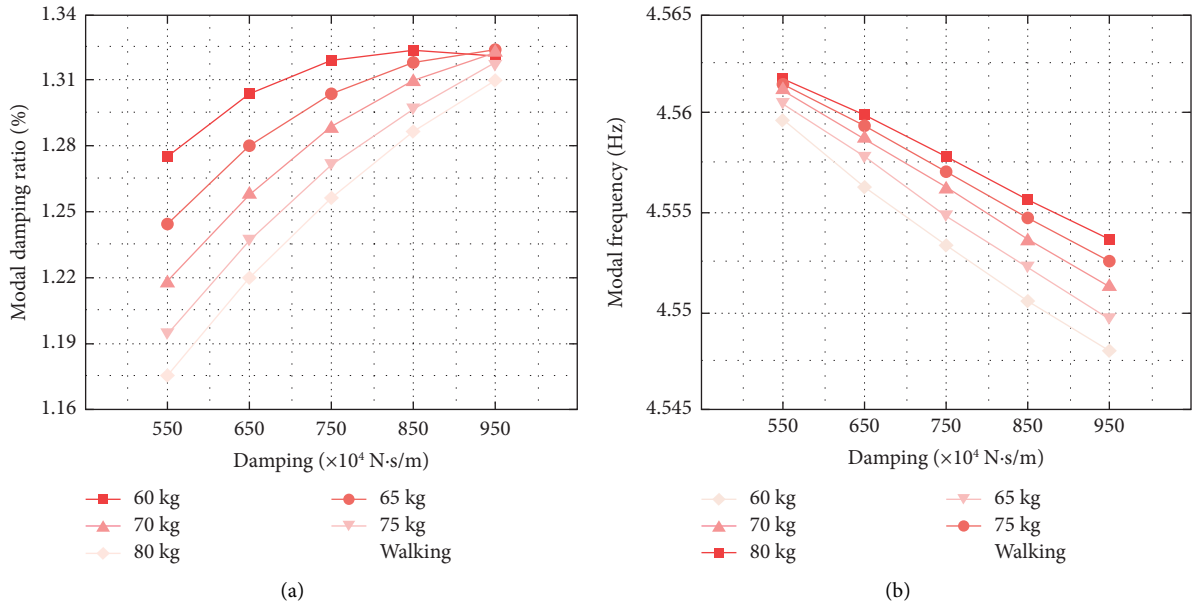

Figure 9: The influence of pedestrian damping on structural modal parameters in pedestrian walking state. (a) Modal damping ratio and (b) modal frequency.

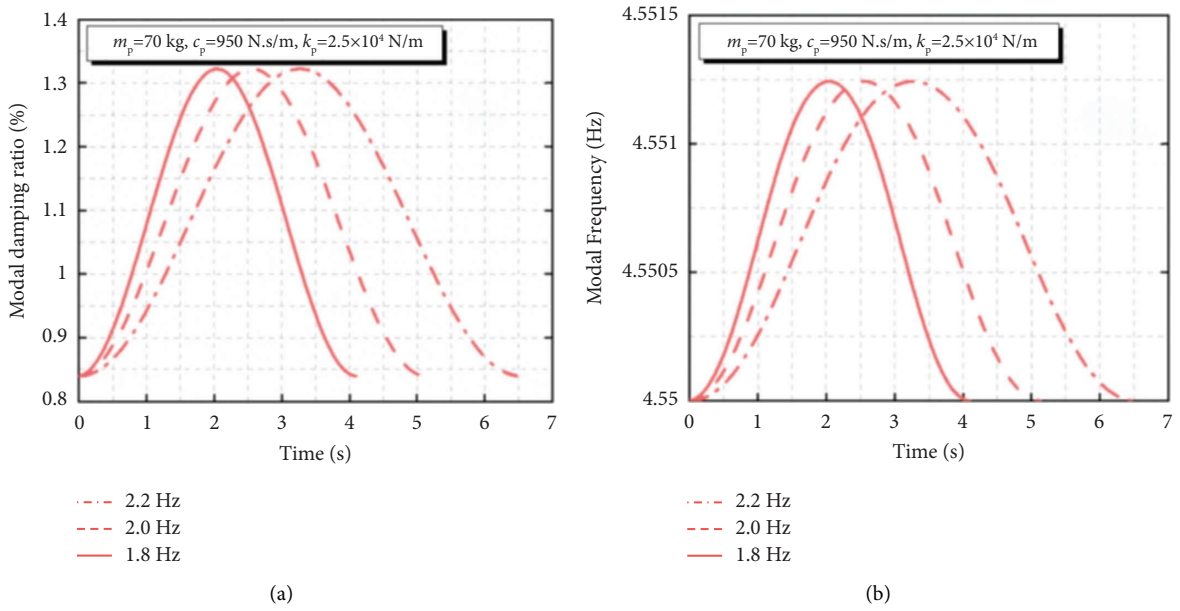

Figure 10: Influence of deterministic pedestrian walking on the floor. (a) Modal damping ratio and (b) modal frequency.

body, the left-right spacing is set at 0.5 m [12], and the front-back spacing is 0.3 m. In the walking state, the position of pedestrians is time-varying, and the time interval Δ_t is taken as 1 s.

(d) According to the time substep d_t, equation (23) is continuously generated and solved step by step. Fourier series model is used for pedestrian walking load and $F_p(t) = G\alpha_v \sin(2\pi f_p t)$, $\alpha_v = 2.5(0.111\ v_p^2 - 0.017\ v_p)$ [10], and α_v is dynamic load factor about walking speed v_p.

4.1.3. Response Analysis. The effects of pedestrian standing position, one-way walking, and two-way walking on structural dynamic parameters were studied. It should be noted that there is no acceleration response analysis under the standing condition.

4.2. Standing Model. The location distribution of pedestrians is shown in Figure 12. Since the span of the floor is 7.7 m × 4.7 m, the maximum crowd density reaches 0.58 p/m^2. It can be seen from Figure 13 that the floor modal

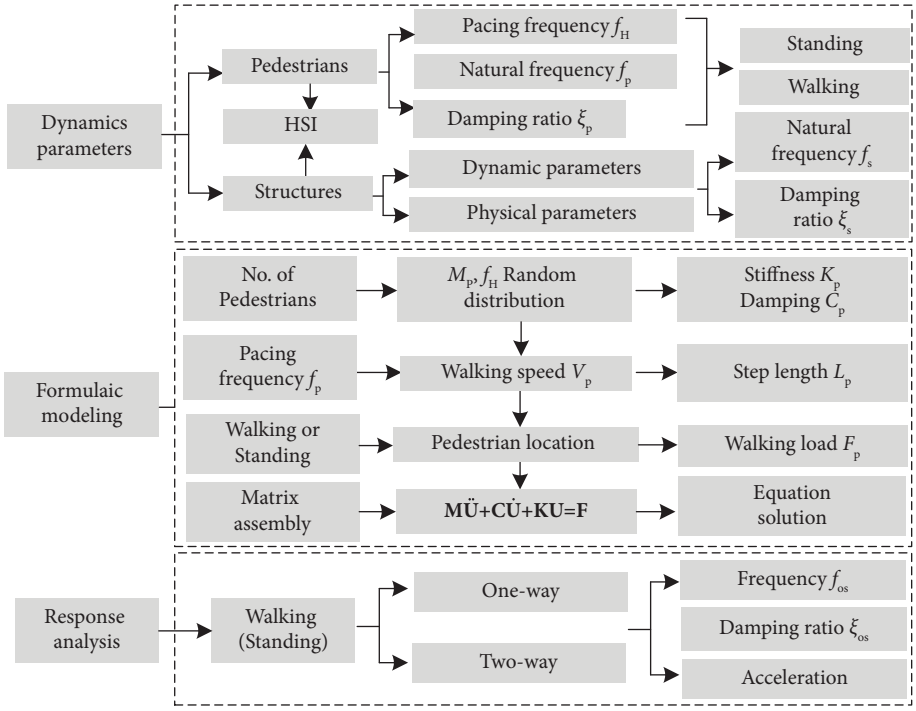

Figure 11: Algorithm of pedestrians walking or standing on the floor.

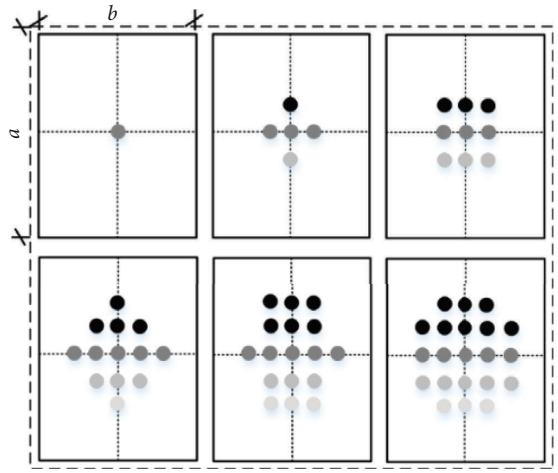

Figure 12: Pedestrian standing area distribution, the number of pedestrians increased from 1 person to 21 people (about 0.58 people/m^2 crowd density), the distance between the left-right is 0.5 m, and the distance between the front-back is 0.3 m.

damping ratio is increasing continuously, but the rising trend gradually slows down with the increase in crowd density. At the same time, the discrete response of the floor modal damping ratio is larger, which is due to the influence of pedestrian randomness. For a crowd of 0.58 p/m^2, the maximum modal damping ratio reaches 8.42%, and the HSI effect is very significant. The floor modal frequency decreases with the increase in crowd density. For the crowd of 0.58 p/m^2, the frequency reduction rate reaches 30%, and the structural dynamic parameters change greatly. When a single person stands in the middle of the floor, the average modal damping ratio and modal frequency of the floor are 1.4% and 4.512 Hz, which are close to the results of the single-person standing test in reference [33].

4.3. One-Way Walking Model. In order to study the influence of pedestrian walking on the floor system, a set of working conditions was designed, as shown in Figure 14. The test number was T1–T6, in which T1–T4 was one-way single-span walking, and the maximum number of pedestrians was 5. Each group of pedestrians gradually differed by 0.6 m span. T5-T6 was one-way double-span walking, with the maximum number of 10 pedestrians. Under the condition of T5, one group of pedestrians walked in the mid-span of the floor; the other group was 1.2 m apart. Under the condition of T6, the average distance between the two groups is 1.2 m, which is located on both sides of the floor. The dynamic parameters such as pedestrian weight, stiffness, and damping have been described in detail in Section 4.1.

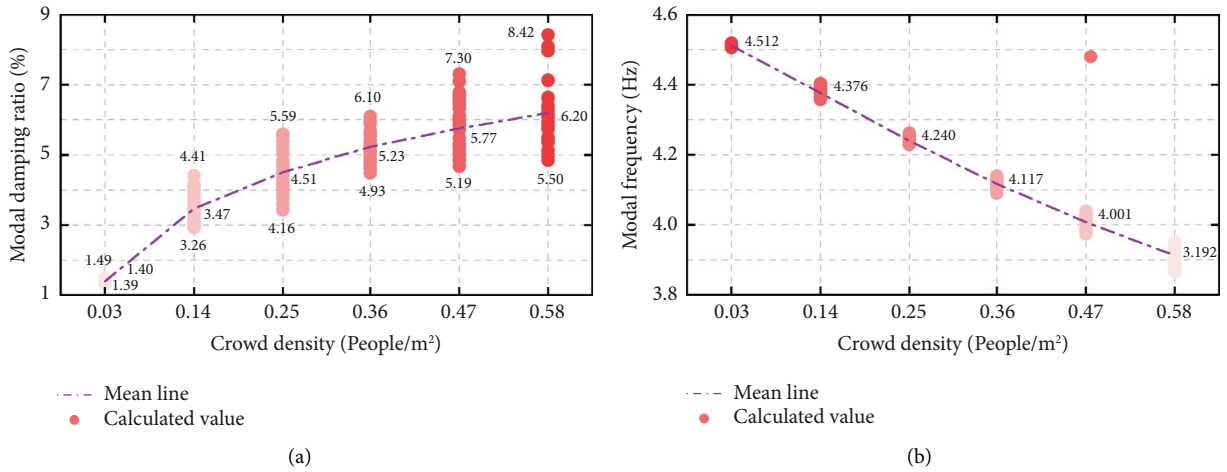

Figure 13: Dynamic parameter response of floor under pedestrian standing. (a) Modal damping ratio and (b) modal frequency.

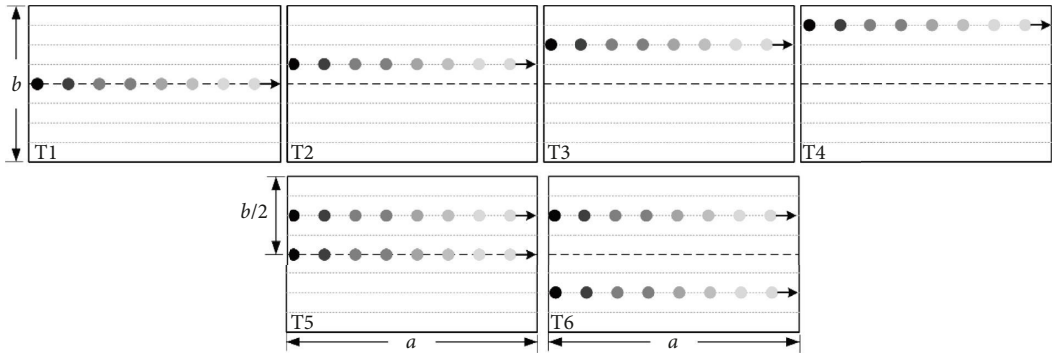

Figure 14: Pedestrian one-way random walking model. (T1) one-way mid-span; (T2) one-way and 0.6 m away from mid-span; (T3) one-way and 1.2 m away from mid-span; (T4) one-way and 1.2 m away from mid-span; (T5) one-way with mid-span and 1.2 m away from mid-span; (T6) one-way and both sides 1.2 m away from the mid-span.

Although the reaching interval of 1 m can be modeled and analyzed [22], considering the function of the metronome and timer in the actual test process, the time interval of pedestrian entering the structure is taken as $\Delta_t = 1$ s. Results of multiple calculations are shown in Figure 15, of which Figures 15(a)–15(d), respectively, show the change trend of the floor modal damping ratio of No. T1–T4. It can be seen from the figures that the increase in pedestrian numbers will lead to an increase in the modal damping ratio, and the discrete effect gradually becomes obvious. Considering the influence of pedestrian randomness, the phenomenon of the discrete effect is in line with the actual situation. By comparing the results of T1–T4, it can be found that the damping ratio of the floor increases with the increase of the number of pedestrians. This is because the T4 condition is far away from the mid-span area of the floor compared with the T1 condition, so the modal damping ratio increases less. Similarly, Figures 15(e)–15(h) show the change in floor system modal frequency under T1–T4 conditions. Generally speaking, the modal frequency of the floor is rising. This change is mainly due to the influence of pedestrian stiffness and pedestrian damping [14, 22, 39]. It is found that the closer to the mid-span region, the more obvious the rise of modal frequency is. Therefore, the lateral width of the floor has an impact on the dynamic response of the floor. Only considering the calculation results of the mid-span area will overestimate the influence of the human-induced vibration and produce unreliable evaluation results.

The growth rate is used to characterize the increase of the modal damping ratio and modal frequency:

$$\beta_\xi = \frac{\left|\max\left(\xi_{os}\right) - \xi_s\right|}{\xi_s},$$
$$\beta_f = \frac{\left|\max\left(f_{os}\right) - f_s\right|}{f_s}, \tag{31}$$

where β_ξ and β_f are the change rates of the modal damping ratio and modal frequency of the floor, respectively. ξ_{os} and f_{os} represent the modal damping ratio and modal frequency of the coupled system under pedestrian walking. It can be seen from Figures 5 and 8 that ξ_{os} and f_{os} are time-varying, so only the peak value is taken for analysis. ξ_s and f_s are the initial damping ratio and natural frequency of the floor. The change rate is shown in Figure 16. Under the condition of T1, the growth rate of 5 pedestrians walking reaches 181%,

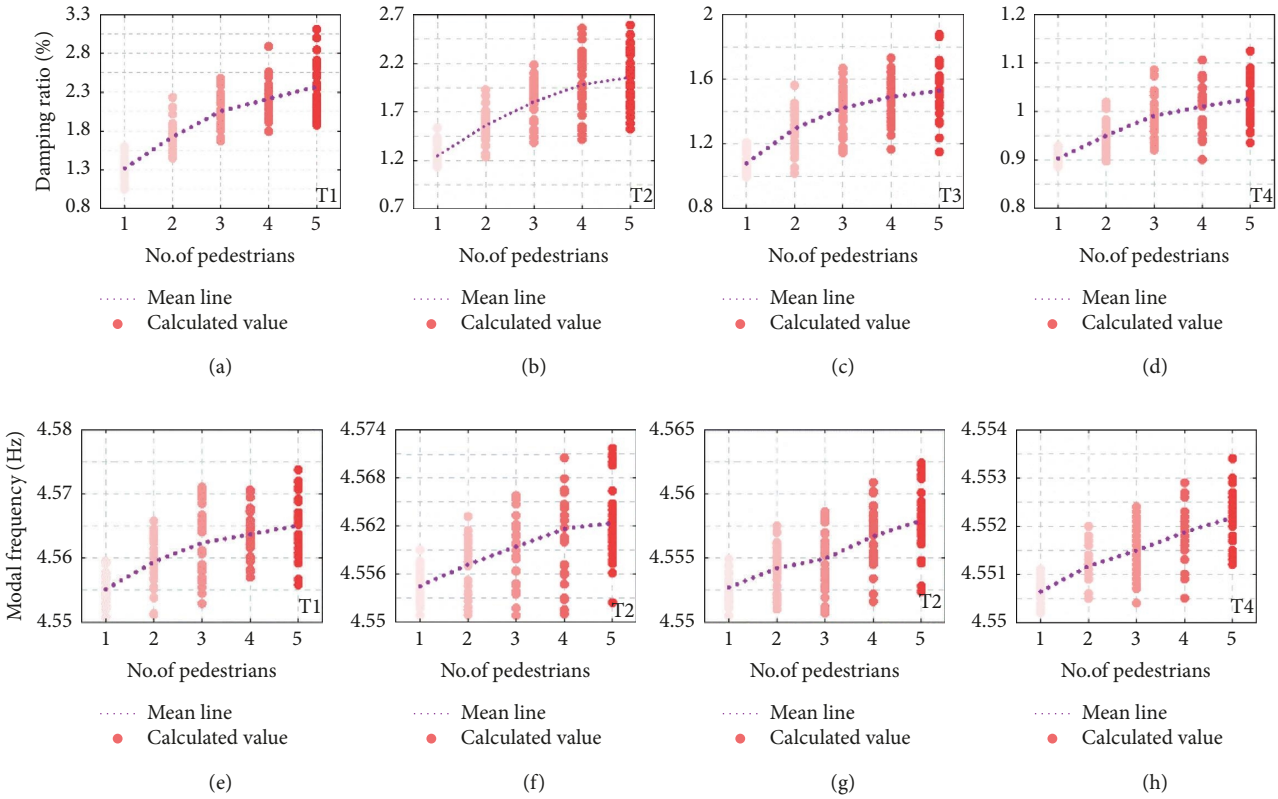

Figure 15: Dynamic parameters of the floor under one-way random walking. (a–d) Modal damping ratio (T1–T4); (e, h) modal frequency.

and the corresponding growth rate is only 22% under T4 condition. The growth rate under the T1 condition reaches 57%, but the T4 condition is only 7% for one-person walking. It can be seen that the influence of the lateral width of the floor structure cannot be ignored. Figure 16(b) shows the growth rate of the floor modal frequency. Due to the small human-structure mass ratio, the frequency change is far less obvious than the change in damping ratio. Under T1 condition, 5 pedestrians walking only increases by 0.33%. Compared with the influence of pedestrians standing in Figure 13(b), it can be found that the influence is very small.

Results of one-way double-span pedestrian walking in T5-T6 conditions are shown in Figures 17 and 18. The number of pedestrians increases from 2 to 10. It can be found that although the floor damping ratio is generally on the rise. The modal frequency of the floor is not monotonically increased, but the modal frequency decreases. Although the number of occurrences is relatively small, this is not mentioned in previous studies. Because of the large sample size, this paper has an advantage in modal frequency analysis. It can be seen from Figures 17(b) and 18(b) that with the increase of the pedestrian number, the amplitude of modal frequency increase or decrease is also gradually obvious. By comparing and analyzing Figures 17(b) and 18(b), it can be found that the change degree of modal frequency decrease or increase under the T6 condition is less than that under the T5 condition. This is mainly due to the fact that pedestrians are more and more far away from the mid-span area of floor under T6 condition. In the case of the floor modal damping ratio, both T5 and T6 conditions increase gradually with the increase in pedestrian number. The average value of floor modal damping ratio under T5 condition is greater than that under T6 condition, which is also because the distribution of pedestrians under T5 is close to the mid-span region.

4.4. Two-Way Walking Model. T7 and T8 conditions are designed to study the influence of two-way walking on floor dynamic parameters. The walking diagram is shown in Figure 19. In the T7 condition, one group of pedestrians walked along the mid-span of the floor, and the other group of pedestrians gathered 1.2 m to walk in the opposite direction. In the T8 model, two groups of pedestrians walk in opposite directions at a distance of 1.2 meters from the mid-span position of the floor. The modal damping ratio and modal frequency are shown in Figures 20 and 21. The variation law of the floor dynamic parameters is similar to that of T5 and T6 conditions. The difference is that the response value of the floor under two-way walking is slightly lower than that of one-way multispan walking. When 10 pedestrians walk on the floor, the average values of floor modal damping ratios calculated by T5 and T6 are 3.1% and 2.3%, respectively. While the average values of floor modal damping ratios calculated by T7 and T8 are 2.9% and 2.2%, the maximum difference between the modal damping ratios is less than 6.9%.

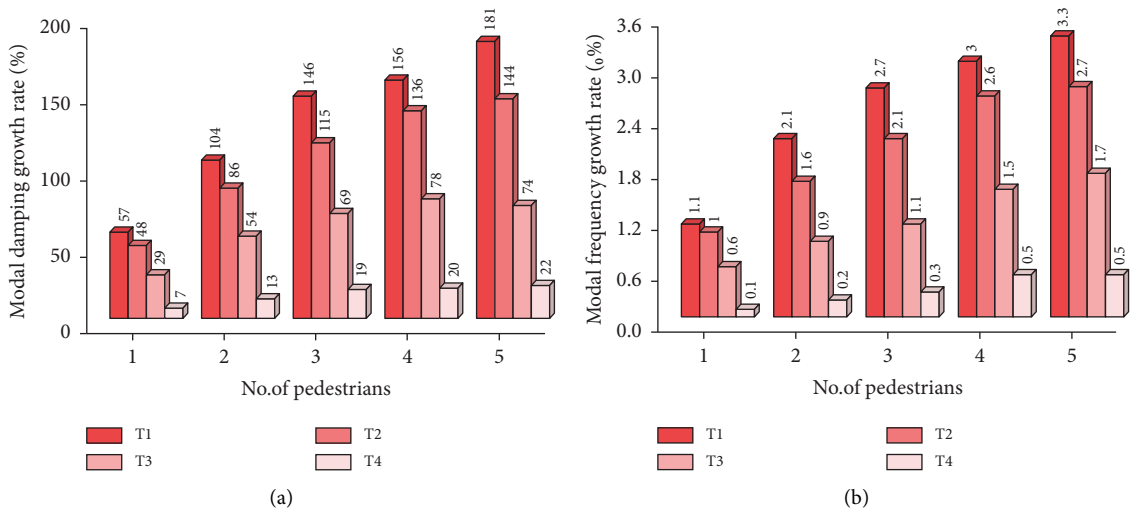

FIGURE 16: Growth rates of the dynamic parameters of the floor under one-way walking. (a) β_ξ. (b) β_f.

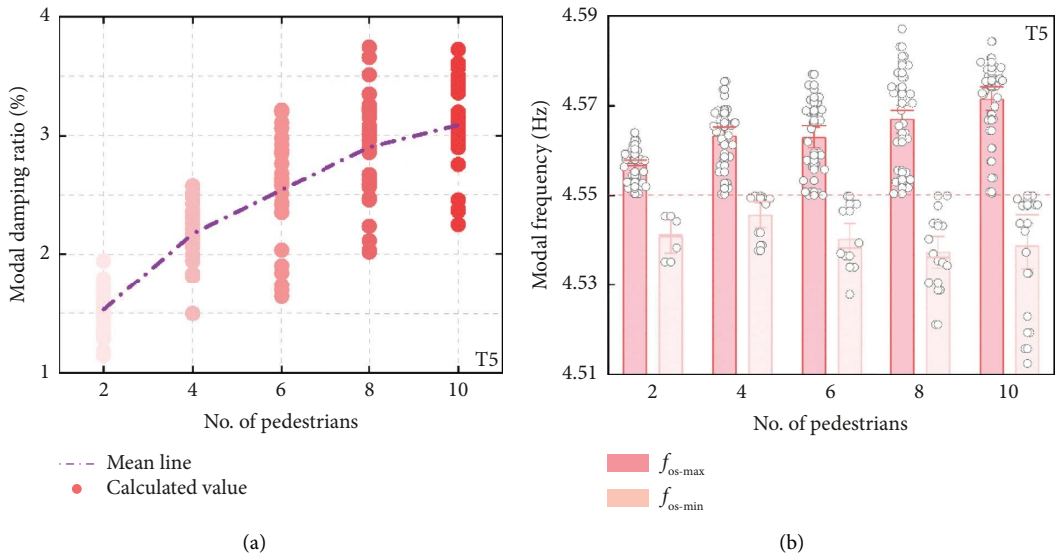

FIGURE 17: Dynamic parameters of the floor under T5 condition. (a) Modal damping ratio and (b) modal frequency.

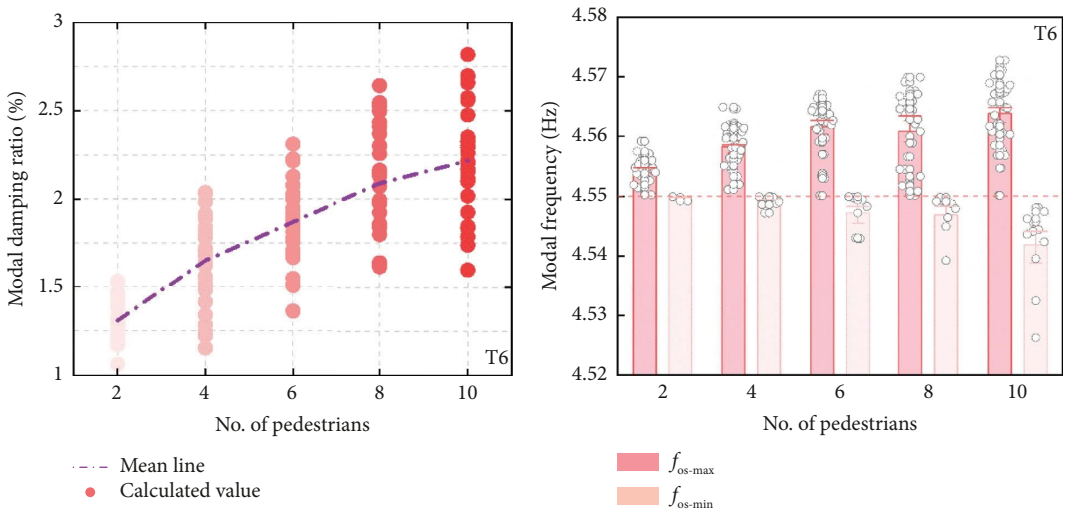

FIGURE 18: Dynamic parameters of the floor under T6 condition. (a) Modal damping ratio and (b) modal frequency.

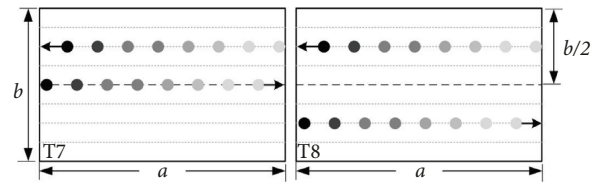

Figure 19: Pedestrian two-way random model.

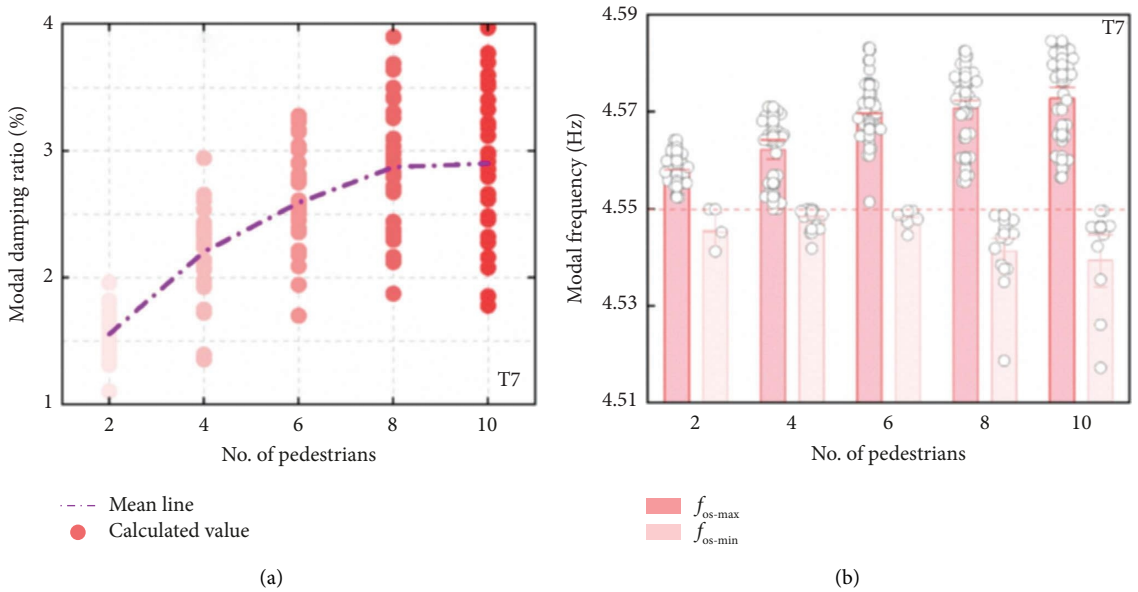

Figure 20: Dynamic parameters of the floor under T7 condition. (a) Modal damping ratio and (b) modal frequency.

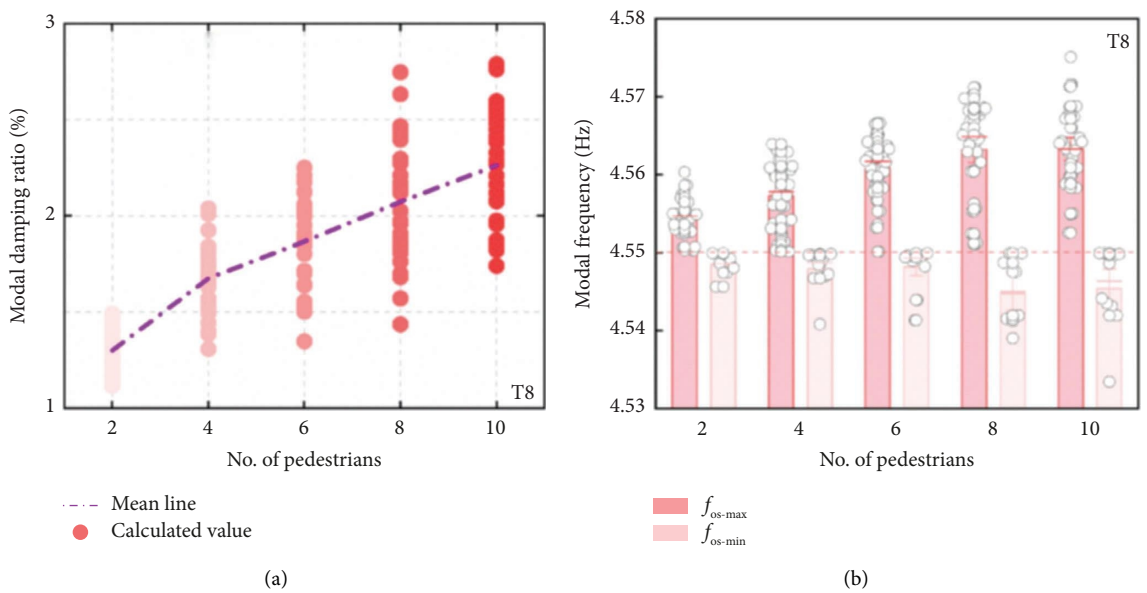

Figure 21: Dynamic parameters of the floor under T8 condition. (a) Modal damping ratio and (b) modal frequency.

The acceleration response of two-way walking on the floor is analyzed, and the variation range of the maximum acceleration with a 95% guarantee rate and the maximum root mean square acceleration of about 1 s are given. The calculation results are shown in Table 5. Under T7 condition, the average maximum acceleration for 10 pedestrians

Table 5: Acceleration response intervals of the floor with 95% guarantee rate.

Mode	No. of pedestrians	Maximum acceleration (m/s^2)		Maximum 1 s-RMS (m/s^2)	
		95 guarantee rates	Mean	95 guarantee rates	Mean
T7	2	[0.087, 0.245]	0.160	[0.047, 0.156]	0.092
	4	[0.101, 0.267]	0.167	[0.052, 0.166]	0.097
	6	[0.107, 0.375]	0.222	[0.056, 0.216]	0.124
	8	[0.128, 0.408]	0.232	[0.064, 0.252]	0.131
	10	[0.127, 0.424]	0.241	[0.056, 0.229]	0.132
T8	2	[0.061, 0.259]	0.139	[0.034, 0.144]	0.081
	4	[0.074, 0.313]	0.177	[0.046, 0.175]	0.104
	6	[0.125, 0.378]	0.207	[0.053, 0.248]	0.115
	8	[0.12, 0.394]	0.214	[0.051, 0.246]	0.12
	10	[0.117, 0.424]	0.217	[0.059, 0.287]	0.12

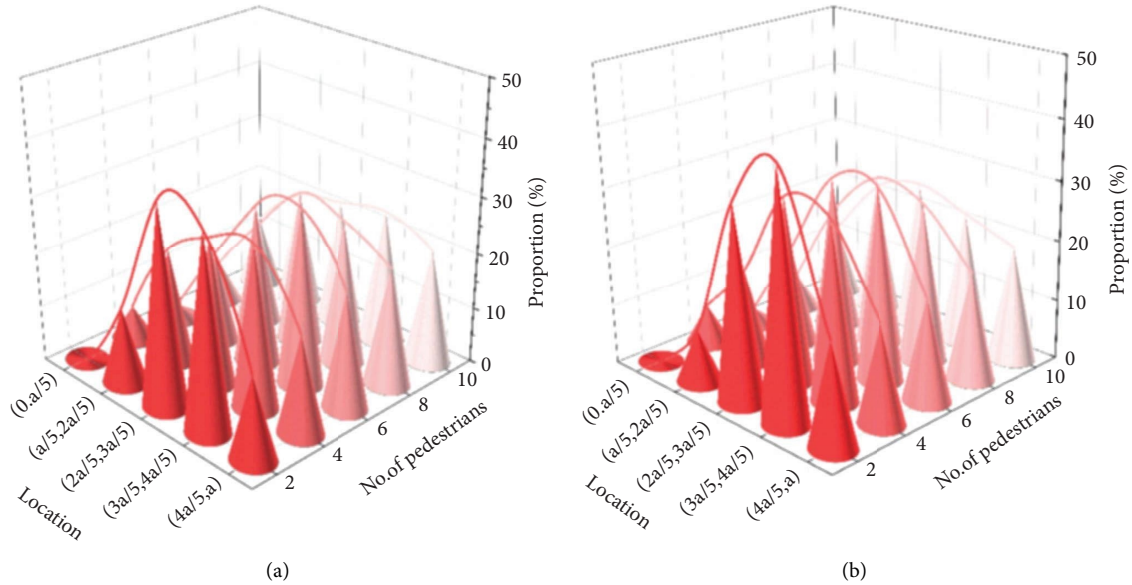

Figure 22: Pedestrian distribution area at maximum acceleration on the floor. (a) Under the T7 condition and (b) under the T8 condition.

random walking is 0.241 m/s^2, and the average value of 1s-RMS is 0.132 m/s^2. Under the T8 condition, the average value of the maximum acceleration for 10 pedestrians random walking is 0.217 m/s^2, and 1s-RMS is 0.12 m/s^2. It can be seen that the acceleration values meet the vibration comfort requirements given in the specification [1, 3].

In order to analyze the position distribution of pedestrians when the structure generates the maximum acceleration, the local distribution of pedestrians is recorded every time the floor generates the maximum acceleration. Figure 22(a) shows the pedestrian distribution under T7 conditions. It can be seen that in the case of two pedestrians, the pedestrian distribution is mainly concentrated near the mid-span area, similar to the normal distribution curve. In the floor area (0, a/5) (a is the length of the long side of the floor), there is no pedestrian distribution when the maximum acceleration is generated. As the number of pedestrians increases, the curve gradually becomes flat. When it reaches a group of 10 pedestrians, the pedestrians are mainly concentrated in the area (a/5, 2a/5), (2a/5, 3a/5), and (3a/5, 4a/5). In these three areas, the proportions of pedestrians are close. This is mainly because the increase in the number of pedestrians has led to the gradual crowding of pedestrians. Figure 22(b) indicates that with the increase in the number of pedestrians, the pedestrian distribution spreads to both sides of the floor middle-span area when the maximum acceleration is generated. According to the code [3], the estimation of the human-induced vibration acceleration response should be calculated with a uniformly distributed load. According to the calculated results in Figure 22, the two sides of the mid-span floor area can be used for uniformly distributed load layout, such as in the area [2a/5, 4a/5] for calculating the dynamic response.

5. Conclusions

For the analysis of a random crowd standing and walking on the floor, the main conclusions are as follows:

(1) When the pedestrians stand on the floor, compared with the initial state of the floor structure, the floor modal damping ratio increases and the modal

frequency decreases. With the increase in pedestrian stiffness, the increase in the damping ratio gradually decreases, and the decrease in frequency gradually increases. As the pedestrian damping increases, the increase in the amplitude of the damping ratio gradually decreases.

(2) When pedestrians walk along the floor, the floor modal damping increases significantly. With the increase in pedestrian stiffness, the rise amplitudes of the floor damping ratio and frequency increase gradually, while with the increase in pedestrian damping, the increase amplitudes of the floor damping ratio and the floor frequency decrease gradually.

(3) Under the action of one-way multispan walking, the floor damping ratio increases, and the modal frequency no longer increases monotonously, but decreases. The floor dynamic parameters under two-way multispan walking are similar to those of one-way multispan. With the increase in the number of pedestrians, when the maximum acceleration occurs, the pedestrian distribution diffuses to both sides of the floor midspan area. Structural acceleration response analysis can take the structure [2a/5, 4a/5] area for uniform load analysis.

Data Availability

The data presented in this study are available upon request from the corresponding author.

Conflicts of Interest

The authors declare that they have no conflicts of interest.

Acknowledgments

The authors acknowledge the funding support of the National Natural Science Foundation of China (Grant nos. 51778462 and 52078368).

References

[1] Hivoss, *EN03- 2007. Design of Footbridges Background Document*, Human Induced Vibration of Steel Structure, Berlin, Germany, 2008.

[2] Ministry of Housing and Urban-Rural Development of the People's Republic of China, *GB/T 51228-2017; Standard for Vibration Load of Buildings*, Ministry of Housing and Urban-Rural Development of the People's Republic of China, Beijing, China, 2018.

[3] Iso, *ISO10137:2007; Bases for Design of Structures-Serviceability of Buildings and Walkways against Vibration*, International Organization for standardization, Geneva, Switzerland, 2007.

[4] Bsi, *National Annex to Eurocode 1: Actions on Structures Part 2: Traffic Loads on Bridges, NA to BS EN 1991-2:2003*, British Standards Institution, London, UK, 2008.

[5] Ministry of Housing and Urban-Rural Development of the People's Republic of China, *GB 50010-2010; Code for Design of concrete Structures*, Ministry of Housing and Urban-Rural Development of the People's Republic of China, Beijing, China, 2015.

[6] P. Young, "Improved floor vibration prediction methodologies," *ARUP Vibration Seminar*, vol. 4, 2001.

[7] J. G. da Silva, S. A. de Andrade, and E. Lopes, "Parametric modelling of the dynamic behaviour of a steel–concrete composite floor," *Engineering Structures*, vol. 75, pp. 327–339, 2014.

[8] S. Zivanovic, A. Pavić, and P. Reynolds, "Vibration serviceability of footbridges under human-induced excitation: a literature review," *Journal of Sound and Vibration*, vol. 279, no. 1-2, pp. 1–74, 2005.

[9] S. Zivanovic, A. Pavić, and P. Reynolds, "Probability-based prediction of multi-mode vibration response to walking excitation," *Engineering Structures*, vol. 29, no. 6, pp. 942–954, 2007.

[10] P. Archbold and B. Mullarney, "Modelling the vertical loads applied by pedestrians at a range of walking velocities," *Australian Journal of Basic and Applied Sciences*, vol. 7, no. 5, pp. 266–277, 2013.

[11] E. Bassoli and L. Vincenzi, "Parameter calibration of a social force model for the crowd-induced vibrations of footbridges," *Frontiers in Built Environment*, vol. 7, Article ID 656799, 2021.

[12] F. Venuti, V. Racic, and A. Corbetta, "Modelling framework for dynamic interaction between multiple pedestrians and vertical vibrations of footbridges," *Journal of Sound and Vibration*, vol. 379, pp. 245–263, 2016.

[13] L. Bruno and A. Corbetta, "Uncertainties in crowd dynamic loading of footbridges: a novel multi-scale model of pedestrian traffic," *Engineering Structures*, vol. 147, pp. 545–566, 2017.

[14] E. Shahabpoor, A. Pavic, and V. Racic, "Interaction between walking humans and structures in vertical direction: a literature review," *Shock and Vibration*, vol. 2016, Article ID 3430285, 22 pages, 2016.

[15] J. Chen, "A review of human-induced loads Study," *Journal of Vibration and Shock*, vol. 36, no. 23, pp. 1–9, 2017.

[16] D. Helbing, L. Buzna, A. Johansson, and T. Werner, "Self-organized pedestrian crowd dynamics: experiments, simulations, and design solutions," *Transportation Science*, vol. 39, no. 1, pp. 1–24, 2005.

[17] D. Helbing and P. Molnar, "Social force model for pedestrian dynamics," *Physical Review A*, vol. 51, no. 5, pp. 4282–4286, 1995.

[18] D. Helbing, I. Farkas, and T. Vicsek, "Simulating dynamical features of escape panic," *Nature*, vol. 407, no. 6803, pp. 487–490, 2000.

[19] B. Fu and X. Wei, "An intelligent analysis method for human-induced vibration of concrete footbridges," *International Journal of Structural Stability and Dynamics*, vol. 21, no. 01, pp. 2150013–2150026, 2020.

[20] X. Wei, "A simplified method to account for human-human interaction in the prediction of pedestrian-induced vibrations," *Structural Control and Health Monitoring*, vol. 28, no. 7, p. e2753, 2021.

[21] X. Wei, J. Liu, and S. Bi, "Uncertainty quantification and propagation of crowd behaviour effects on pedestrian-induced vibrations of footbridges," *Mechanical Systems and Signal Processing*, vol. 167, Article ID 108557, 2022.

[22] C. Caprani and E. Ahmadi, "Formulation of human-structure interaction system models for vertical vibration," *Journal of Sound and Vibration*, vol. 377, pp. 346–367, 2016.

[23] E. Shahabpoor, A. Pavic, and V. Racic, "Identification of mass–spring–damper model of walking humans," *Structures*, vol. 5, pp. 233–246, 2016.
[24] E. Ahmadi, C. Caprani, and A. Heidarpour, "An equivalent moving force model for consideration of human-structure interaction," *Applied Mathematical Modelling*, vol. 51, pp. 526–545, 2017.
[25] E. Shahabpoor and A. Pavic, "Human-structure dynamic interaction during short-distance free falls," *Shock and Vibration*, vol. 2016, Article ID 2108676, 12 pages, 2016.
[26] M. Zhang, C. T. Georgakis, W. Qu, and J. Chen, "SMD model parameters of pedestrians for vertical human-structure interaction," *Dynamics of Civil Structures*, vol. 2, 2015.
[27] L. He, J. Yuan, F. Fan, and C. Liu, "Dynamic forces of swaying human and responses of temporary demountable grandstand based on experiment and simulation," *Shock and Vibration*, vol. 2018, Article ID 2791491, 22 pages, 2018.
[28] S. Živanović, *Probability-based Estimation of Vibration for Pedestrian Structures Due to Walking*, University of Sheffield, Sheffield, England, 2006.
[29] Z. Y. Cao, *Vibration Theory of Plates and Shells*, China Railway Publishing House, Beijing, China, 1983.
[30] O. Kopmaz and S. Telli, "Free vibrations of a rectangular plate carrying a distributed mass," *Journal of Sound and Vibration*, vol. 251, no. 1, pp. 39–57, 2002.
[31] J. W. Nicholson and L. A. Bergman, "Free vibration of combined dynamical systems," *Journal of Engineering Mechanics*, vol. 112, no. 1, pp. 1–13, 1986.
[32] E. Shahabpoor, A. Pavic, and V. Racic, "Using MSD model to simulate human-structure interaction during walking," *Topics in Dynamics of Civil Structures*, Springer, New York, NY, USA, 2013.
[33] Z. Yang, *Study on Parameter Identification and Vibration Control for Large-Span Floors Base on Crowd Load*, Southeast University, Dhaka, Bangladesh, 2017.
[34] E. Shahabpoor, A. Pavic, V. Racic, and S. Zivanovic, "Effect of group walking traffic on dynamic properties of pedestrian structures," *Journal of Sound and Vibration*, vol. 387, pp. 207–225, 2017.
[35] X. Zheng and J. Brownjohn, "Modeling and simulation of human-floor system under vertical vibration," in *Proceedings of Spie the International Society for Optical Engineering*, Newport Beach, CA, USA, August 2001.
[36] F. Silva and R. Pimentel, "Biodynamic walking model for vibration serviceability of footbridges in vertical direction," in *Proceeding of the 8th International Conference on Structural Dynamics*, Leuven, Belgium, July 2011.
[37] L. L. Cao, *Research on Human-Induced Vibration Response and Vibration Control of Long-Span Floor in High-Speed Railway Waiting Hall*, Southeast University, Dhaka, Bangladesh, 2016.
[38] F. Venuti and L. Bruno, "An interpretative model of the pedestrian fundamental relation," *Comptes Rendus Mecanique*, vol. 335, no. 4, pp. 194–200, 2007.
[39] G. Busca, A. Cappellini, S. Manzoni, M. Tarabini, and M. Vanali, "Quantification of changes in modal parameters due to the presence of passive people on a slender structure," *Journal of Sound and Vibration*, vol. 333, no. 21, pp. 5641–5652, 2014.